The 18th World Conference on Seismic Isolation, Energy Dissipation, and Active Vibration Control of Structures (18WCSI)
Antalya, Turkey, November 2023

High-performance Japanese dynamic testing system for seismic isolation: E-Isolation

Yoshiharu Takahashi[1], Toru Takeuchi[2], Shoichi Kishiki[2], Yozo Shinozaki[3], Masako Yoneda[2], Koichi Kajiwara[4], and Akira Wada[2*]

[1] Kyoto University, Kyoto, Japan
[2] Tokyo Institute of technology, Tokyo, Japan
[3] Taisei corporation, Tokyo, Japan
[4]NIED, Tsukuba, Japan
*wada@akira-wada.com

Abstract. The dynamic characteristics of seismic isolation bearings, the key elements for seismically isolated structures, are highly dependent on the size effect and rate-of-loading, especially under extreme loading conditions. Therefore, confirming the actual properties and performance of these bearings with full-scale specimens under prescribed dynamic loading protocols is essential. However, the number of testing facilities with such capacity is still limited and even though the existing labs are conducting these tests, their dynamic loading test setups are subjected to friction generated by the large vertical loads and inertial force of the heavy table which affect the accuracy of measured forces. To solve this problem, the authors have proposed a direct reaction force measuring system that can eliminate the effects of friction and inertia forces, and a seismic isolation testing facility with the proposed system (E-isolation) have been completed in March 2023 in Japan. This test facility is designed to conduct not only dynamic loading tests of seismic isolation bearings and dampers but also to perform hybrid simulations of seismically isolated structures. In this paper, the design concepts, and the realization of this system into an actual dynamic test facility are presented through the reduced-scale mock-up tests using the proposed system.

Keywords: Seismic Isolation, Isolation Bearing, Dynamic test, Friction, Inertia force, Scale effect, E-Isolation

1 Dynamic testing system eliminating friction and inertia forces

1.1 The proposed system

Since the latter half of the 20th century, seismic isolation and vibration control techniques have been developed and put into practical use by challenging researchers and engineers worldwide, and after more than 40 years, they are now used in thousands of buildings, private residences, highways in many seismic areas in the world. Seismic isolation and vibration control methods can keep the structures undamaged even in a major earthquake and realize continuous occupancy.

Among the typical rubber bearings used for seismic isolation, natural rubber-based laminated rubber bearings have a relatively linear stress–strain relationship, while lead-plugged rubber bearings, high-damping rubber bearings, and friction-type bearings with additional damping functions are known to exhibit complex behavior under high axial forces and large dynamic deformations, and also depend on the size of the bearing. The numerical modeling of these bearings is complicated due to their size, velocity, pressure, and temperature dependence. Therefore, it is very important to verify the behavior of seismic isolation bearings using full-scale dynamic test facilities. However, there has been no facility in Japan that can dynamically evaluate full-scale bearings larger than 800 mm in diameter, such as those used in large buildings and bridges, and such performance tests have been relied upon at test facilities outside Japan, such as those in the United States and Taiwan. Fig. 1a shows the configuration of a typical seismic isolator test facility such as the Seismic Response Modification Device (SRMD) at UCSD [2]. The moving platen that shears the specimen is moved dynamically in the horizontal direction while being subjected to vertical forces of tens of thousands of kilonewtons. However, the frictional forces caused by the large vertical force and the inertial force of the heavy platen are mixed into the measured reaction force of the load cell attached to the horizontal dynamic jack. Although friction models that consider the effects of velocity and pressure have been proposed and provided based on the studies such as [1], [3], [4], it is still not easy to accurately reproduce a complex friction model that depends on the individual test machine conditions, and the time delay involved in the calculation is a challenge for real-time hybrid simulation experiments.

To solve this problem, the authors have proposed a new type of reaction force measurement system [7], as shown in Fig. 1b, where a reaction beam was placed on top of

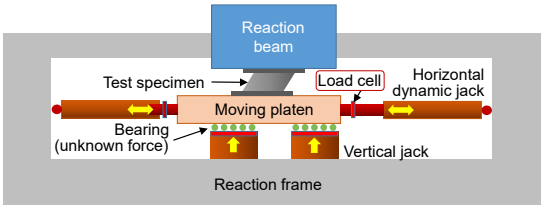

(a) Conventional reaction force measurement system

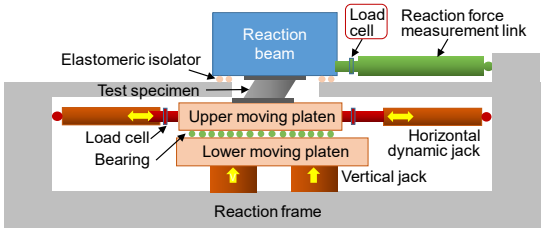

(b) Proposed reaction force measurement system

Fig. 1 Conventional and proposed measurement system

the specimen, which is elastically supported with extremely low stiffness in the horizontal direction and almost rigid in the vertical direction, and the rigid reaction force measurement links are connected to the reaction beam in the horizontal direction. Most of the horizontal reaction force is measured in real-time using these force measurement links, and because the reaction beam hardly moves, almost no inertial force is generated. Furthermore, by supporting the reaction beam with elastomeric isolators, which are soft in the horizontal direction and rigid in the vertical direction, only 1–2% of the horizontal force transmitted through these elastomeric isolators which can be accurately calculated by their measured deformation.

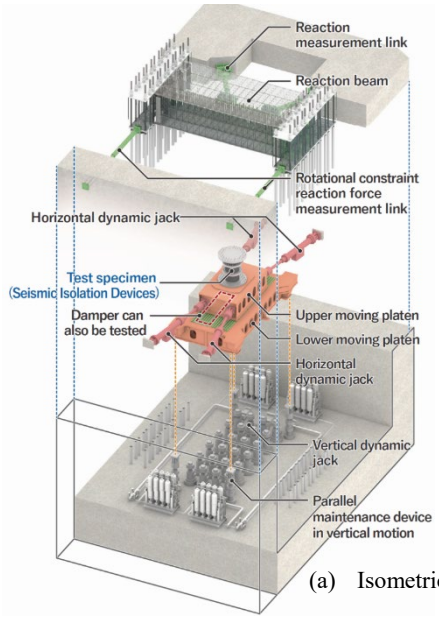

(a) Isometric view

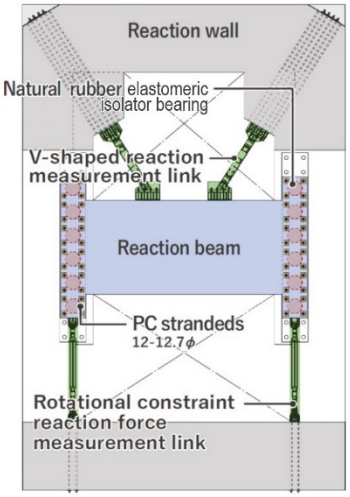

(b) Plan

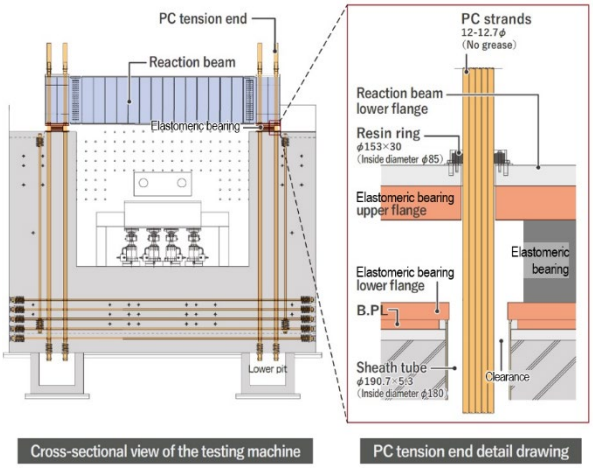

(c) Section and fixing detail of the reaction beam

Fig.2 Configurations of the planned testing facility

The configuration of the testing facility incorporating the proposed system is outlined in Fig. 2 a-c. The new testing facility planned in Japan, Hyogo, Miki besides E-defense facility has a vertical load capacity of 36,000kN (static), 30,000kN (dynamic), stroke limit of 250mm and velocity capacity of 70mm/sec. In the horizontal direction, dynamic single directional loading capacity is 6,500kN (static), 5,100kN (dynamic) with ±1,300mm stroke limit and the max velocity is 800mm/sec. In this testing system, a big steel reaction beam is placed above the specimen similar to the SRMD facility in UCSD, but in this case it is supported by laminated natural rubber bearings with low horizontal stiffness and high vertical stiffness, instead of being fixed to the RC reaction walls. The reaction beam is connected to a horizontally rigid RC reaction wall by a V-shaped measurement link with built-in load cells and a couple of rotational-constraint measurement links with built-in load cells. The two transverse beams at both sides of the reaction beam are pulled down with horizontally-free PC strands of 14.6m length between the bottom and top anchors that apply compressive force to the laminated rubber bearings so that the compression force on these bearings is not lost even when the reaction beams are subjected to lift-up effects during the experiments. Because of the low horizontal stiffness of the rubber bearings supporting the reaction beam, majority of the horizontal force is measured through the reaction measurement link, where the ratio of horizontal force transmitted through the laminated rubber bearings is less than 1%. Due to the reliable elastic characteristics of the laminated natural rubber bearings, horizontal forces in these bearings can be accurately included in the resultant reaction forces by using their horizontal deformation. Since the horizontal displacement of the reaction beam is expected to be in the vicinity of 1-2 mm and acceleration is at a negligible level, the measured forces should not be affected by the frictional or inertial forces, which have been an issue in existing facilities.

1.2 Reduced-scale mock-up experiment

To verify the practicality of the proposed reaction force measurement system, dynamic-loading experiments were performed using a reduced-scale setup. The experiment was conducted using a dynamic test frame located at the Tokyo Institute of Technology. The test setup is shown in Fig. 3. This test frame was equipped with a horizontal dynamic jack that can apply loading in one direction and a moving platen supported by two linear sliders. The horizontal dynamic jack had a maximum load capacity of 500 kN, maximum velocity of 500 mm/s, and maximum positive and negative amplitudes of ± 300 mm. Because there was no existing vertical-loading device in this frame, it was newly installed for this test. The test set-up consists of, from bottom to top, a moving platen, the specimen, a vertical force apparatus, and a reaction beam. V-shaped horizontal reaction force measurement links with the load cells were attached to the side of the reaction beam, and the reaction beam was supported by elastomeric isolators (laminated natural rubber bearings) attached to the bottom beam. The reaction beam was tightly connected to the bottom beam by eight PC-steel rods, and the initially applied tension exceeded 1600 kN so that the elastomeric isolators supporting the reaction beam will not lift up. The ends of the PC-steel rods were anchored using rotational nuts and remained horizontally movable. These configurations are equivalent to those of the

proposed full-scale apparatus shown in Fig. 1b. The only difference was that the vertical-loading system was located above the specimen, including the load-cell measuring the vertical force also placed at the reaction side.

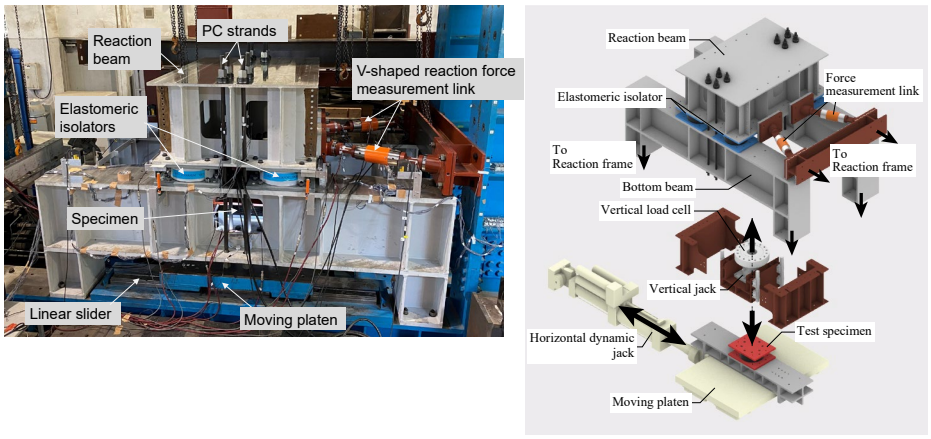

Fig. 3 Setup for reduced-scale mock-up experiment

When designing a force measurement link, the shear force and bending moment caused by the vertical displacement of the reaction beam must be maintained within the allowable range of the load cell included in the force measurement link. Therefore, the hinges at both ends of the force measurement links must have high axial stiffness, but low rotational stiffness. In this experiment the force measurement links with a narrowed flat section (hereinafter referred to as "elastic pin") were implemented and compared. Fig.4 shows pictures of the force measurement links with elastic pins.

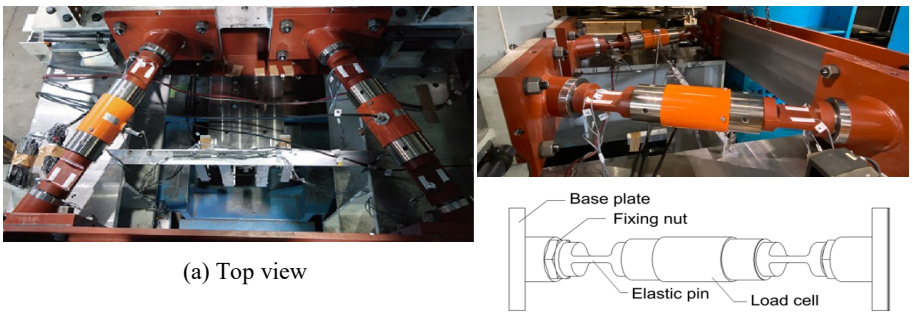

(a) Top view

(b) Side view

Fig. 4 Force measurement link with elastic pin

The horizontal reaction force R_1 in the proposed reaction force measurement system was obtained as the sum of the horizontal component of the forces acting on the load cell with V-shaped force measurement links, horizontal force calculated from the deformation of the four elastomeric isolators supporting the reaction beam, and PΔ force

due to the initial tension of the PC-steel bar binding the reaction beam.

$$R_1 = -(N_{L-A} + N_{L-B}) \cdot \cos\theta + (4k' + k_{P\Delta}) \cdot \left(\frac{\delta_7 + \delta_8 + \delta_9 + \delta_{10}}{4} \right) \quad (1)$$

where the angle between the V-shaped links and the loading direction θ = 23.9°, the horizontal stiffness k' = 0.58 kN/mm (G = 0.39, B-type) for the bearing under small deformation, and the PΔ stiffness $k_{P\Delta}$ = 1.14 kN/mm as a result of the pre-tension in the PC-steel rods. The reaction force measured by the load cell attached to the horizontal jack is defined as R_2. As a reference, the horizontal reaction force R_3 was calculated from the horizontal stiffness k of the laminated rubber specimen according to the manufacturer catalog (stiffness at 100% shear strain) and the shear deformation. Three types of 300 mm diameter laminated natural rubber bearing specimens from different manufacturers and shear modulus were used as the subjects of dynamic cyclic loading tests.

Fig.5 shows the relationship between the horizontal deformation and horizontal reaction force for the tests with quasi-static (f = 0.05 Hz) loading, compression stress σ = 0 MPa, and amplitudes A = ± 2, 20, and 100 mm. Because the loading velocity was low and no vertical pressure was applied, inertial and frictional forces that could cause measurement errors were not generated, and the results indicated that R_1 and R_2 were close. In addition, in the medium-amplitude range, the linear stiffness indicated by the green line (R_3) is generally in agreement with the stiffness at 100% shear strain (corresponding to 58.5mm shear deformation). The measured stiffness was slightly higher for lower amplitudes of A=2mm and lower in higher amplitudes of A=100mm.

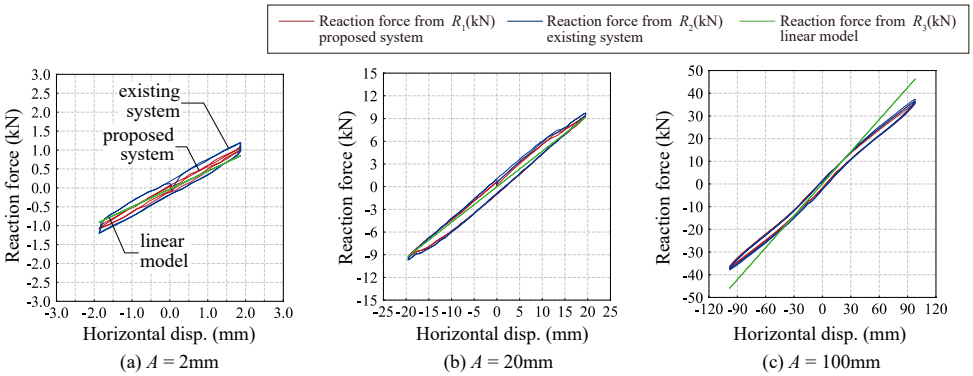

(a) A = 2mm (b) A = 20mm (c) A = 100mm

Fig.5 Reaction force- deformation relationship: quasi-static (f=0.05Hz) loading, no-compression

Fig. 6 shows the horizontal displacement-horizontal reaction force relationship at amplitudes of A = ± 2, 20, and 100 mm at a frequency f = 1.0 Hz, where the loading velocity is increased while maintaining the compression stress σ = 0 MPa. It can be observed from these graphs that errors were generated between R_1 and R_2. These errors increased with acceleration as the sinusoidal amplitude increased, which can be explained by the inertial force being proportional to the acceleration.

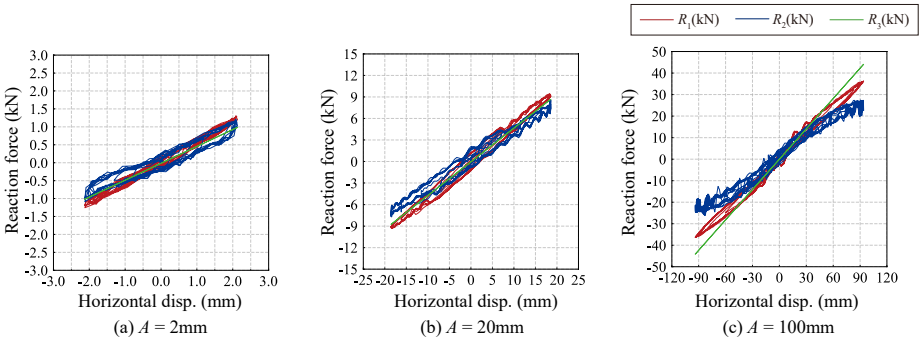

Fig.6 Reaction force- deformation relationship: dynamic loading (f =1.0 Hz), no-compression

Fig.7 shows the horizontal deformation-horizontal reaction force relationship for amplitudes A = ± 2, 20, and 100 mm at a compression stress of σ =15 MPa under quasi-static loading. It can be seen from these plots that there is a large error between R_1 and R_2, especially in the small amplitudes due to the frictional force between the moving platen and linear sliders, which is proportional to the compression. The frictional force was maintained between 6 and 9 kN. Because the vertical load was 100 kN, the linear slider had a friction coefficient equivalent to μ=0.06-0.09. In Figure 7b, a reaction spike was observed near the zero displacement in R2 graph. This was attributed to the slight denting in the linear slider surface of this particular test setup caused by numerous preliminary compression tests.

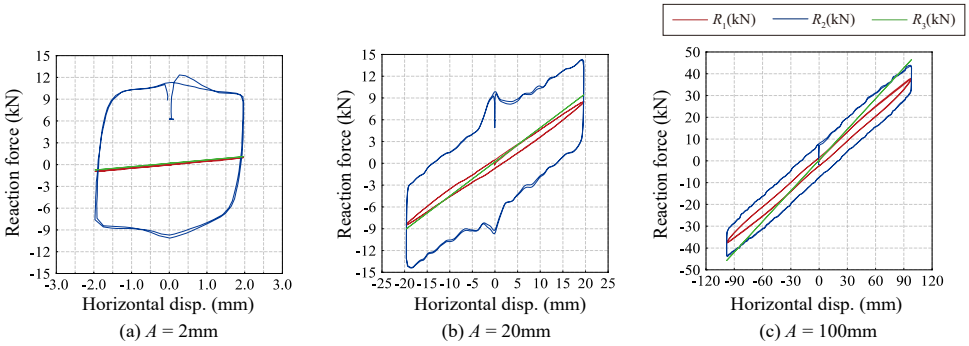

Fig. 7 Reaction force-deformation relationship:
quasi-static (f=0.05Hz) loading, with 15MPa compression

Finally, Fig. 8 shows the horizontal reaction force-horizontal deformation–relationship for f = 1 Hz, σ = 15 MPa, and amplitudes A = ± 2, 20, and 100 mm, with dynamic loading and vertical load. In these graphs, the influence of the inertial force shown in Fig. 6 and that of the friction force shown in Fig. 7 coexist. From Fig. 6–8, the measured values of the proposed measurement links are stable and unaffected by friction and inertial forces, even in a small deformation range.

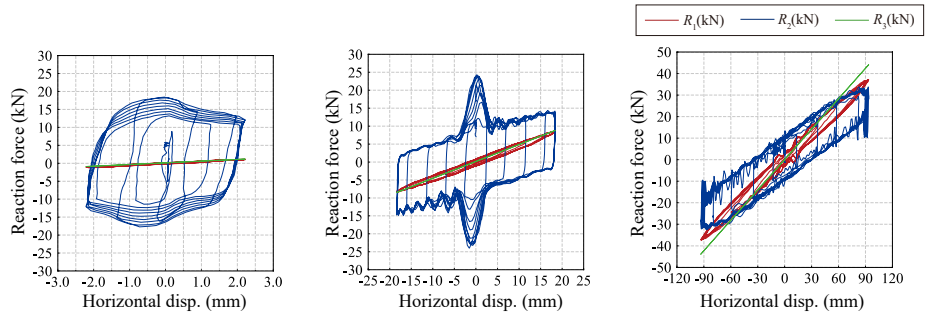

Fig.8 Reaction force-deformation relationship:
dynamic loading (f =1.0 Hz), with 15MPa compression

Fig. 9 shows examples from hybrid simulation [5],[6] results of a seismically isolated two-story building using the reduced-scale mock-up experimental setup and a rubber bearing specimen. In the figure, the red line indicates the response results of the hybrid simulation using the proposed measurement system, and the blue line is using the load cell at the horizontal dynamic jack, which includes the friction force. The dotted green line is the pure response analysis, which estimates the rubber isolator bearing as linear stiffness. The red line is more accurate, reflecting the precise nonlinear hysteresis of the rubber bearing, which indicates a more realistic response. While the result with the existing system shows significant error due to contamination of the frictional forces.

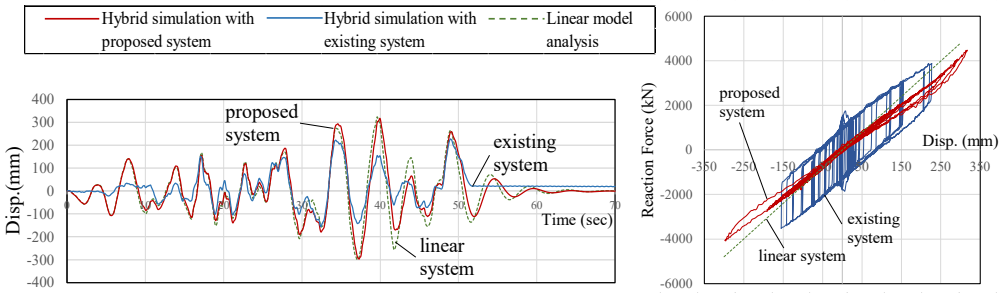

Fig.9 Hybrid simulation example using the proposed measurement system vs. existing system

From those reduced-scale mock-up tests and simulations, the proposed force measurement system was found to be effective through various dynamic conditions of vertical pressure and frequency with an error of less than 1%. On the other hand, the conventional dynamic jack load cell measuring the reaction force was heavily affected by the inertial force under dynamic loading and frictional force when exposed to a vertical force.

2 Construction of the testing facility

In the following, the detailed design and construction of real-size testing facility is described.

2-1 Design and construction of RC reaction wall

A part of the design drawings of RC reaction wall and construction plan are shown in Fig.10. For a future extension to 50,000kN vertical loading capacity with a two-dimensional horizontal moving platen, the RC reaction wall has been designed to withstand these conditions with 9.90-11.00m clear span. The thickness of the reaction walls is 3.5m and the foundation thickness is 4.5m. Prestressing is implemented in the foundation and walls, for preventing cracks in these concrete walls.

The reaction beam is placed on the RC reaction walls supported through twelve laminated natural rubber bearings with 650mm diameter. PC strand sets consisting of twelve strands with 12.7mm diameter are connecting the reaction beam onto the RC reaction walls. Four of these PC strand sets are provided for each bearing with a design prestress level of 1050kN on each (1240kN in construction, considering future relaxation). Pre-stressing forces are designed to keep the support rubber bearings under compression even under the most severe testing conditions.

To allow the expected horizontal movement of the reaction beam, PC strands have been placed in sheath tubes with 190.7mm diameter. 5.3mm thickness, allowing 47mm clearance in the design stage around the PC strands. The 11.52m tall sheath tubes are precisely installed into the RC reaction walls within 1/650 error margin, using template frameworks as shown in Fig. 11a. As a result, 30mm clearance around the PC strands is secured (Fig. 11b).

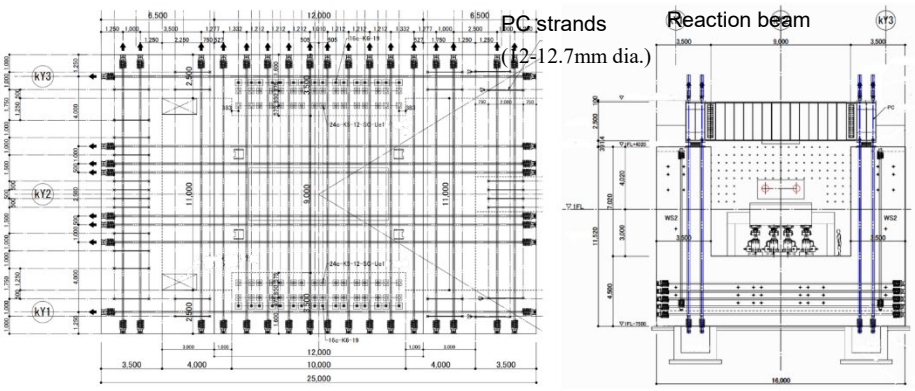

Fig. 10 Plan and section of RC reaction wall with PC strand arrangement (Courtesy of Kurosawa Kensetsu)

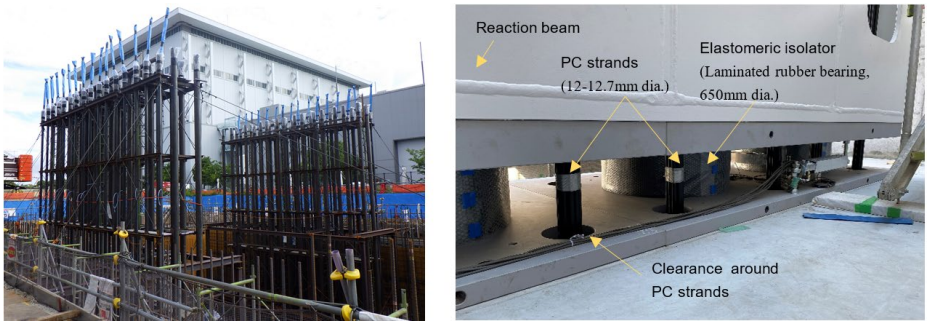

(a) Template framework for sheath tube (b) PC strands and elastomeric bearing supporting reaction beam

Fig. 11 PC strands construction anchoring the reaction beam

2.2 Design and fabrication of steel reaction beam

The reaction beam consists of four steel box beams with section of 2.5 m height, 1.2 m wide, 9.1m long, 22 mm to 30 mm in thickness and 20 tons weight, and two more box-shaped beams of 1.25 m wide, 7.2 m long and 22 tons weight on each end connected in an H-shaped plan, as shown in Fig. 12. The six beams are transported individually and assembled at the construction site by friction bolt connections. In addition, large steel plates of 30mm of 4.8m width and 8.4m length are bolted on the top and bottom of the connected boxes for integration. In design it was confirmed that each component was kept below the allowable stress level for the steel material and slip load of the bolts, where the design vertical deformation was 7.6mm (1/1450), and the torsional angle was 1/759 under vertical load of 30,000kN and horizontal load of 6,000kN.

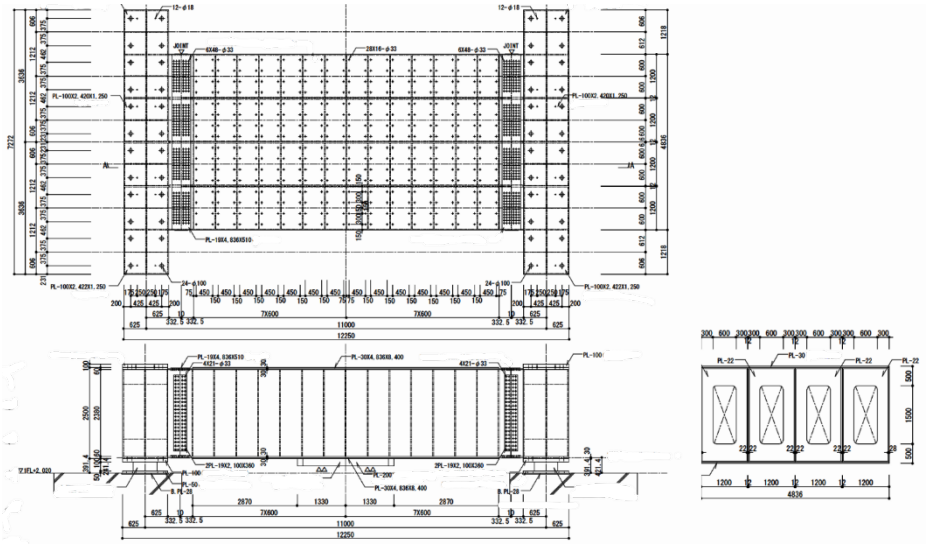

Fig. 12 Plan and section of reaction beam (Courtesy of Nippon Steel Engineering and Dr. Hidemoto Mukai)

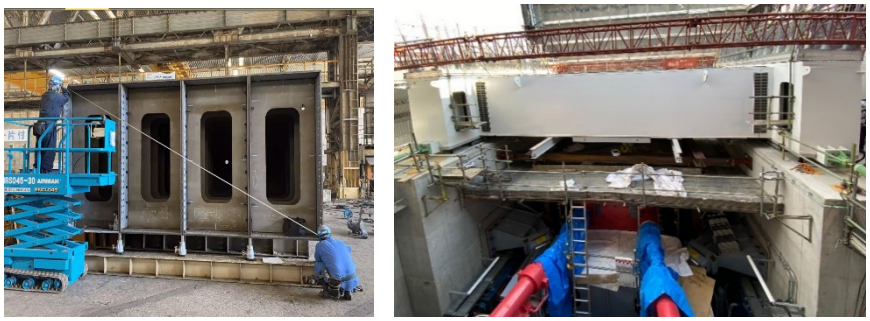

(a) Fabrication of reaction beam (b) Installed reaction beam on elastomeric bearings

Fig. 13 Fabrication and installation of reaction beam

To ensure the quality of each friction bolt connection, comprehensive tolerance controls were conducted during the fabrication of the reaction beam. During the assembly, the warping caused by welding was minimized and the tolerance of the friction joint was successfully obtained to be less than 1 mm (Fig.13).

2.3 Elastomeric isolator supporting reaction beam

Twelve 650-mm-diameter natural rubber laminated bearings (rubber shear modulus G=0.39N/mm^2, horizontal stiffness for small amplitudes k=1.1 kN/mm, total stiffness of 12 bearings is 13.2 kN/mm) were employed for supporting the reaction beam as in Fig. 14a. Sliding bearings such as ball bearings or hydrostatic bearings generate frictional reaction forces, which fluctuate instantaneously and frequently depending on the phase of motion, making it difficult to determine the friction forces by using displacement data. Conversely, natural rubber isolator bearings exhibit relatively low horizontal stiffness, and as long as linear behavior is ensured, the reaction force can be accurately determined from the very small displacement (Fig. 14b). Micro-deformation experiments were conducted on candidate laminated rubber bearings during the design stage to confirm the stability of their linear behavior.

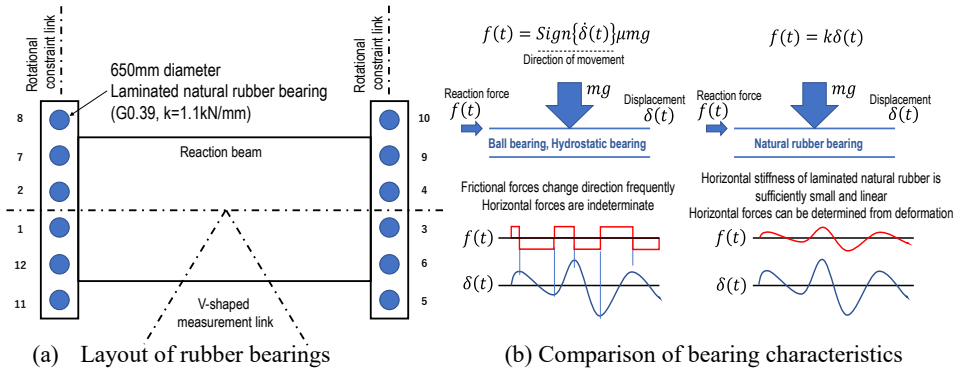

(a) Layout of rubber bearings (b) Comparison of bearing characteristics

Fig.14 Elastomeric isolator supporting the reaction beam

Besides, 48 PC strands of 12m×5/6 (fixed ends)-effective length (4 strands per support) between the bottom of the reaction beam and the bottom of RC wall with 1240 kN of tension force each exhibit a horizontal stiffness of 6.0 kN/mm in total due to their PΔ effect. As a result, total horizontal stiffness at supporting bearings is expected to be approximately 19kN/mm only. Therefore, the horizontal forces induced by these bearings are expected to be substantially small relative to the measurement links, namely less than 1%, and can be accurately evaluated by measuring the horizontal displacement of the reaction beam, which is approximately 1-2mm under maximum force 6,000kN.

2.4 Configuration of the moving platen

As shown in Fig. 15 and 16, the moving platen consists of a lower layer that moves vertically and an upper layer that moves horizontally in the x-direction. The lower platen is controlled by 24 vertical dynamic jacks while the upper platen is supported on the lower layer by linear sliders with 18 rails and 14 sliders on each rail (total number of the sliders of 252), moves in the x-direction by 4 horizontal dynamic jacks.

As the vertical jacks are simply supporting the moving platens, there is no restraining measure against partial uplift as a result of the rotation about y-axis and x-axis. Also, they do not resist against z-axis rotation or y-axis displacements. Therefore, 4 leveling jacks restrain x-axis and y-axis rotations, and 4 backup arms are provided to limit z-axis rotation and movement in the y-axis. Furthermore, 4 horizontal dynamic jacks are angled slightly (10° from the x-axis) to control y-axis movement and z-axis rotations.

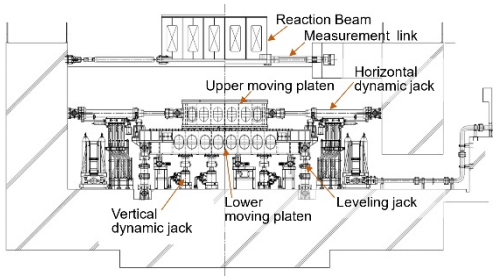

(a) X-dir. section of the test facility

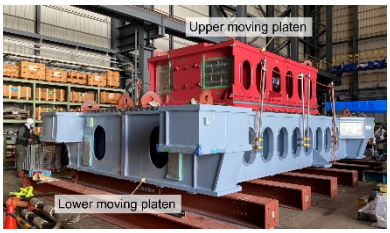

(b) Upper and lower moving platen

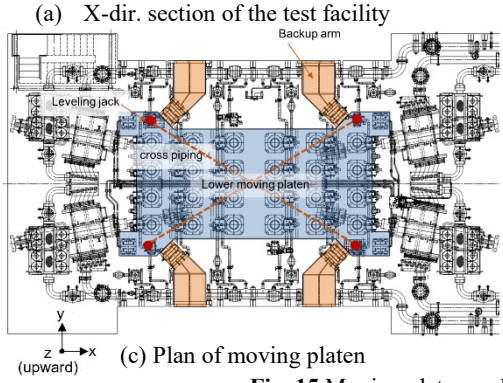

(c) Plan of moving platen

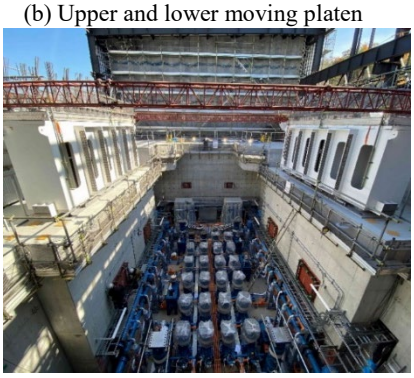

(d) 24 vertical dynamic jacks

Fig. 15 Moving platen and vertical dynamic jacks

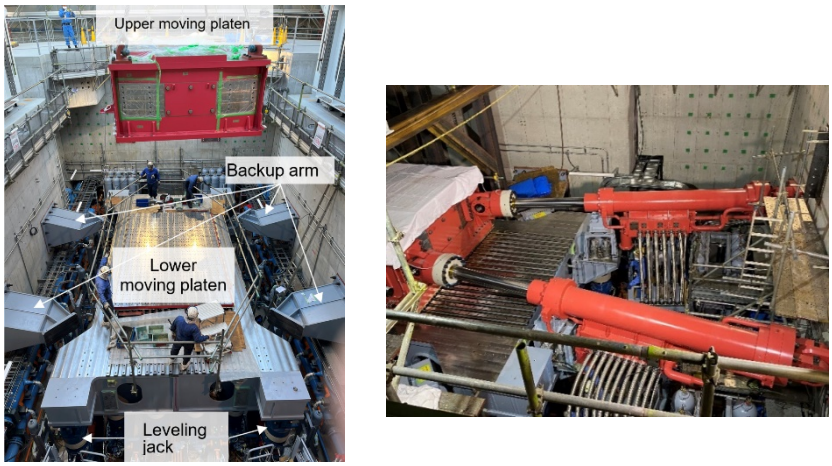

(a) Leveling jack and backup arm (b) Horizontal dynamic jacks

Fig. 16 Moving platen and dynamic jacks-2

The leveling jacks are linked with cross-connected oil chambers which stabilize the horizontal level without obstructing the vertical movement of the mechanism. Total 28 numbers of vertical load cells are provided on the vertical jacks and leveling jacks, and total vertical reaction force (F_z), rotational moment around x-axis (M_x) and rotational moment around y-axis (M_y) can be obtained from these values.

2.4 Design and fabrication of force measurement links

The reaction force measurement link, consists of a V-shaped measurement link intersecting the center of the reaction beam and a couple of rotational constraint measurement links, as shown in Fig. 17.4MN and 1.5MN load cells are mounted on the V-shaped link, and the rotational constraint link, respectively. V-shaped measurement links restrain the displacement of the reaction beam in the x and y directions, and the individual reaction forces along x and y directions can be obtained by multiplying cosine and sine components on axial forces, respectively. To restrain the rotation of the reaction beam about the z-axis, a couple of rotational constraint links are added between both wings of the reaction beam and the RC reaction wall. Conducted analyses indicate that up to 75% of the major reaction forces will be resisted by the V-shaped measurement links and the remaining by the rotational constraint links. The additional reaction forces measured by these links are expected to be 99%.

V-shaped link should be able to keep up with the vertical displacement of the center of the reaction beam under a vertical force of 30,000 kN within the elastic range, as same as the reduced scale mock-up experiment setup. Therefore, joints with reduced bending stiffness at both ends (elastic pins) are used for these links.

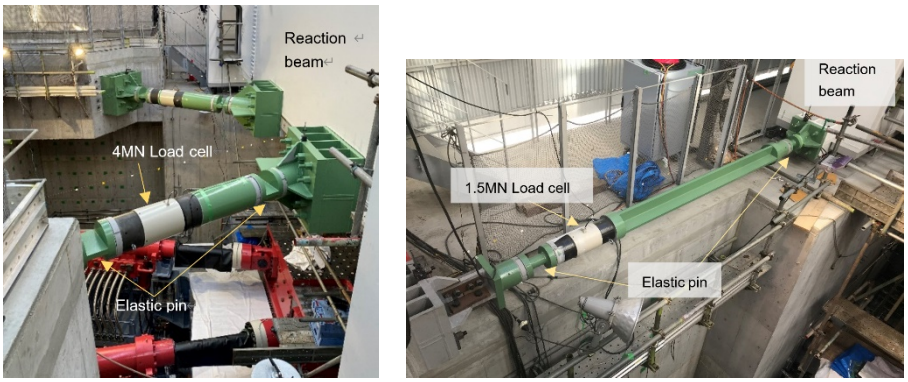

(a) V-shaped measurement link (b) Rotational constraint link

Fig. 17 Reaction-force measurement link

2.5 Test jigs for various specimens

Testing jig for seismic isolation bearings and energy-dissipation devices are shown in Fig. 18a-c. Not only seismic isolation bearings but short column specimens up to 2.1m in height can also be assessed by this testing device. For energy-dissipation devices, an additional load-cell unit consisting of three flat load-cells is attached to the RC reaction wall (Fig. 18b), and by setting the specimen between this load-cell unit and upper moving platen, reaction forces will be directly measured eliminating the effects of friction and inertia forces similar to the measurement link system (Fig. 18c).

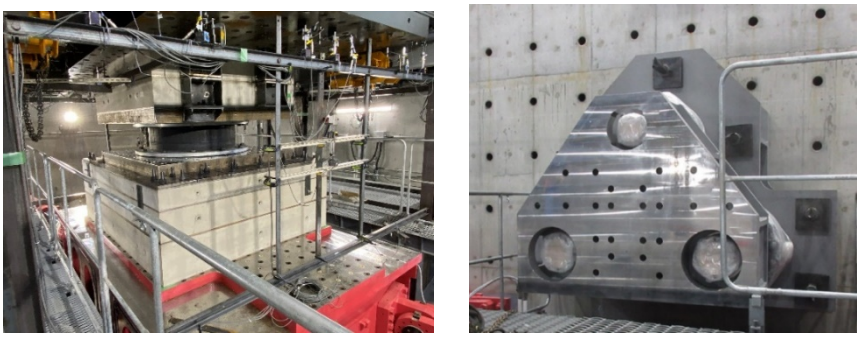

(a) Test jig for seismic isolation bearings (b) Test jig for energy-dissipation devices

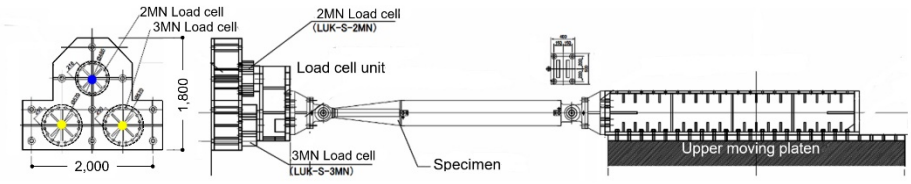

(c) Set-up for energy-dissipation devices

Fig. 18 Testing jig for various specimens

2.6 Building design

The E-isolation test facility building is composed of the main test block, including the test machine and hydraulic source plant, and the office block, including the measurement room and the observatory office. The interior of the observatory office is designed with timber details, providing a relaxed atmosphere for the researchers and visitors. The construction has been completed in March 2023.

Fig. 19 Exterior view and interior of E-isolation

3. Conclusions

In this article, a recently-constructed dynamic testing facility in Japan, E-isolation, specifically designed for seismic isolation bearing tests, eliminating the effects of friction and inertia forces was introduced. Presented discussions are summarized as follows.

1) The proposed system that eliminates the contamination of frictional and inertial forces mixing into the measured reaction forces in the dynamic test systems by using a direct measurement link that measures the reaction force was explained.

2) The performance of the proposed concept was confirmed using a reduced-scale mock-up test experiment, and the substantial accuracy of friction and inertia force elimination method was confirmed.

3) Design and construction of a full-scale test facility, E-isolation was carried out between early 2022 and the end of March 2023, starting the performance tests for various seismic isolation bearings and energy dissipation devices from April 2023.

References

1. Alireza, S., Schellenberg, A. H., Schoettler, M. J., Mosqueda, G., Mahin, S. Real-time hybrid simulation of seismically isolated structure with full-scale bearings and large computational models, 2019; *CMES*, **120**(3), 693–717. doi.org/10.32604/cmes.2019.04846
2. Benzoni, G., Seible, F.(1998), Design of the Caltrans seismic response modification device (SRMD) test facility, Research co-ordination meeting of the IAEA's co-ordinated research programme on intercomparison of analysis methods for seismically isolated nuclear structures, 1998; 101–115.
3. Constantinou M. C., Tsopelas P., Kasalanati A., and Wolff E. D. (1999). Property Modification Factors for Seismic Isolation Bearings. Technical Report MCEER-99-0012, University of Buffalo, 1999
4. Constantinou, M.C., Whittaker, A.S., Kalpakidis, Y., Fenz, D.M., Warn, G.P.(2007), Performance of seismic isolation hardware under service and seismic loading, Technical Report MCEER-07-0012, University of Buffalo, 2007
5. Schellenberg, A., Kim, H. K., Takahashi, Y., Fenves, G. L., Stephen A. Mahin, S. A., *OpenFresco Command Language Manual (Ver.2.6)*, <available at https://openfresco.berkeley.edu/>.
6. Takahashi, Y., Fenves (2006), Software framework for distributed experimental-computational simulation of structural systems, *Earthquake Engineering and Structural Dynamics*, 2006; **35**, 267–291. Doi.org/10.1002/eqe.518
7. Takahashi, Y., Takeuchi, T., Kishiki, S., Shinozaki, Y., Yoneda, M., Kajiwara, K., Wada, A.(2023), E-Isolation–High-performance dynamic testing installation for seismic isolation bearings and damping devices, *International Journal of High-rise buildings*, 2023; **12**(1), 93-105, 2023